

# Development of spin fluctuations under the presence of $d$ -wave bond order in cuprate superconductors

Satoshi Ando, Youichi Yamakawa, Seiichiro Onari, Hiroshi Kontani  
*Department of Physics, Nagoya University, Nagoya 464-8602, Japan*  
 (Dated: May 3, 2021)

In cuprate superconductors, superconductivity appears below the CDW transition temperature  $T_{CDW}$ . However, many-body electronic states under the CDW order are still far from understood. Here, we study the development of the spin fluctuations under the presence of  $d$ -wave bond order (BO) with wavevector  $\mathbf{q} = (\pi/2, 0), (0, \pi/2)$ , which is derived from the paramagnon interference mechanism in recent theoretical studies. Based on the  $4 \times 1$  and  $4 \times 4$  cluster Hubbard models, the feedback effects between spin susceptibility and self-energy are calculated self-consistently by using the fluctuation-exchange (FLEX) approximation. It is found that the  $d$ -wave BO leads to a sizable suppression of the nuclear magnetic relaxation rate  $1/T_1$ . In contrast, the reduction in  $T_c$  is small, since the static susceptibility  $\chi^s(\mathbf{Q}_s)$  is affected by the BO just slightly. It is verified that the  $d$ -wave BO scenario is consistent with the experimental electronic properties below  $T_{CDW}$ .

The electronic states in cuprate superconductors have been studied as central issues in condensed matter physics. Especially, the mechanisms and the true order parameters of the charge density wave (CDW) state and the pseudogap state have intensively studied in the last decade. Figure 1(a) shows a schematic phase diagram of Y-based compound (YBCO). The antiferromagnetic (AFM) order at filling  $n = 1$  rapidly disappears with hole doping. For wide doping range, the pseudogap phase appears below  $T^*$ . As discussed in Refs. [1–3], large quasiparticle damping could induce sizable reduction in the density of states (DOS). On the other hand, the rotational symmetry breaking [4–6] and the time reversal symmetry breaking [7] have been observed recently. To explain them, nematic transitions such as  $d$ -wave bond order (BO) [8–10] and charge or spin-loop-current [11–15] are proposed.

Inside the pseudogap region, the CDW-type order emerges below  $T_{CDW}$ , higher than the superconducting transition temperature  $T_c$  [16–35]. Spin-fluctuation scenarios [36–41] and superconducting-fluctuation scenarios [42–45] have been proposed as its driving mechanism. Its wavevector is  $\mathbf{q} = (\delta, 0), (0, \delta)$  with  $\delta \approx \pi/2$  according to the X-ray scattering experiments [16–30] and the STM measurements [31–34]. Conventional CDW with local charge density modulation  $\Delta n_i (\equiv n_i - n_i^0)$  is suppressed by the on-site Coulomb interaction  $U$ . In contrast, off-site order parameters, such as the BO parameter  $\delta t_{ij}$  ( $\propto \langle c_{i\sigma}^\dagger c_{j\sigma} \rangle - \langle c_{i\sigma}^\dagger c_{j\sigma} \rangle_0$ ) are not suppressed by  $U$ . In fact, various multipole orders are induced by the interference mechanism between paramagnons, as revealed by the density wave (DW) equation [9, 10, 46–51], the functional renormalization group (fRG) studies [8, 52–56], and other theories [57, 58]. In Refs. [8, 9], it was predicted that the nematicity in the pseudogap-phase below  $T^*$  is the ferro ( $\mathbf{q} = \mathbf{0}$ )  $d$ -wave BO, and the experimental CDW phase is the antiferro ( $\mathbf{q} = (\delta, 0)$ )  $d$ -wave BO.

In many cuprate superconductors, superconductivity appears under the presence of the CDW-type order.

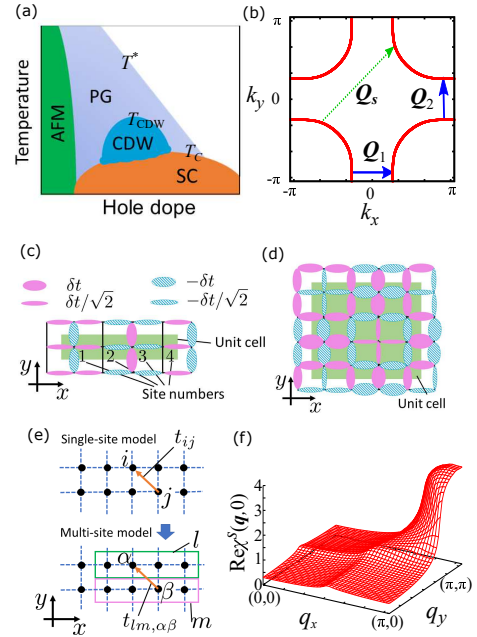


FIG. 1. (a) Schematic phase diagram of YBCO. (b) Original FS.  $\mathbf{Q}_1$  and  $\mathbf{Q}_2$  are the axial nesting vectors related to the period of the BO.  $\mathbf{Q}_s = (\pi, \pi)$  is a nesting vector. (c) Schematic single- $\mathbf{q}$  four-period  $d$ -wave BO.  $\delta t$  is the modulation of the hopping. (d) Schematic double- $\mathbf{q}$   $4 \times 4$  period  $d$ -wave BO. (e) Relation between indices  $i, j$  and  $\alpha, \beta, l, m$ .  $i(j)$  is the site index over all the space.  $\alpha(\beta)$  is the site index in a unit cell  $l(m)$ . (f) Spin susceptibility without the BO at  $T = 0.01$ . It has a peak at  $\mathbf{Q}_s$ .

However, many-body electronic states under the CDW-type order are still far from understood. For example, the Hall and Seebeck coefficients show large positive values for  $T \gg T_{CDW}$  [59, 60], while they suddenly decrease and become negative below  $T_{CDW}$  [61–63]. These observations indicate the Fermi pocket formation due to the band folding by the antiferro BO. Also, the nuclear magnetic relaxation rate  $1/T_1$ , which represents the low-

energy spin-fluctuation strength, is strongly suppressed below  $T_{\text{CDW}}$  [64]. In contrast,  $T_c$  is suppressed by the CDW-type order only slightly in YBCO [27–29], and the finite-energy spin-fluctuation strength (at  $E \sim 30$  meV) grows monotonically even below  $T_{\text{CDW}}$  according to the neutron inelastic scattering experiments [65].

In this paper, we study the development of the spin fluctuations under the presence of antiferro  $d$ -wave BO. Based on the  $4 \times 1$  ( $4 \times 4$ ) cluster Hubbard model with single- $\mathbf{q}$  (double- $\mathbf{q}$ ) BO parameters, we study the feedback effects between spin-fluctuations and self-energy self-consistently by using the fluctuation-exchange (FLEX) approximation [66]. The pseudogap formation due to the  $d$ -wave BO leads to the sizable suppression of  $1/T_1T$ . In contrast, the reduction in  $T_c$  due to the BO remain small, since  $\chi^s(\mathbf{Q}_s)$  is affected by the BO just slightly. It is found that the  $d$ -wave BO scenario naturally explains essential electronic properties below  $T_{\text{CDW}}$  in Fig 1(a).

The present study reveals the importance of the site dependent electronic states under the BO state, because the site averaging approximation (SAA) leads to inappropriate results as we will show later. Therefore, analysis of the cluster Hubbard model is necessary for understanding the electronic states in the BO phase.

The Hubbard Hamiltonian is represented by  $H = H_0 + H_U$ , where the hopping term is  $H_0 = \sum_{\sigma} \sum_{ij} t_{ij} a_{i\sigma}^{\dagger} a_{j\sigma}$ , and the interaction term is  $H_U = \sum_i U a_{i\downarrow}^{\dagger} a_{i\uparrow}^{\dagger} a_{i\uparrow} a_{i\downarrow}$ . Here,  $a_{i\sigma}^{\dagger}$  and  $a_{i\sigma}$  are the creation and annihilation operators of the electron on site  $i$  with spin  $\sigma$ , respectively.  $t_{ij}$  is the transfer integral from site  $j$  to  $i$ . We define  $t_1$ ,  $t_2$ , and  $t_3$  as the first, the second, and the third nearest neighbor hopping without any orders, respectively. Here, we set  $t_1 = -1$ ,  $t_2 = 1/6$ , and  $t_3 = -1/5$ .

Figure 1(b) shows the Fermi surface (FS) without the  $d$ -wave BO. The nesting vector  $\mathbf{Q}_s = (\pi, \pi)$  gives the peak of the spin fluctuation.  $\mathbf{Q}_1 = (\delta, 0)$  and  $\mathbf{Q}_2 = (0, \delta)$  are the axial nesting vectors related to the period of the BO. We set  $\delta = \pi/2$  and  $n = 1.015$  to discuss the four-period order. (We also investigated the five-period ordered case at  $n = 0.888$ , and confirmed that the results are qualitatively similar to those in the four-period ordered case.)

The antiferro  $d$ -wave BO is represented by the modulation of the hopping as

$$\delta t_{ij}^{\mathbf{q}} = \delta t \left[ (\delta_{\mathbf{r}_i - \mathbf{r}_j, \hat{x}} - \delta_{\mathbf{r}_i - \mathbf{r}_j, \hat{y}}) + (i \leftrightarrow j) \right] \times \text{Re} \left[ e^{-i(\mathbf{q} \cdot \frac{\mathbf{r}_i + \mathbf{r}_j}{2} - \gamma)} \right], \quad (1)$$

where  $\delta t_{ij}^{\mathbf{q}}$  has an opposite sign for  $x$ -direction and  $y$ -direction. The period and direction of the modulation are decided by wave number  $\mathbf{q}$ .  $\delta t_{ij}^{\mathbf{Q}_1}$  is shown in Fig. 1(c).  $\mathbf{r}_i$  is the position of site  $i$ , and  $\hat{x}$  ( $\hat{y}$ ) is the  $x$  ( $y$ )-direction unit vector.  $\delta t$  is the BO strength, and we assume that  $\delta t$  has the BCS-like  $T$  dependence,

$\delta t(T) = \delta t_0 \tanh(1.74 \sqrt{T_{\text{BO}}/T - 1})$ .  $T_{\text{BO}}$  is the BO transition temperature, which corresponds to  $T_{\text{CDW}}$ .  $\gamma$  is the phase parameter of the BO. We have confirmed that both  $1/T_1T$  and  $T_c$  are independent of  $\gamma$  as shown in Figs. S1(e) and (f) in the supplemental material (SM), so we set  $\gamma = 0$  in this study. We call  $\delta t_{ij}^{\mathbf{Q}_1}(T)$  in Eq. (1) the “single- $\mathbf{q}$ ” BO.

We also discuss the “double- $\mathbf{q}$ ” BO represented by  $\delta t_{ij}^{\mathbf{Q}_1}(T) + \delta t_{ij}^{\mathbf{Q}_2}(T)$ . Figure 1(d) shows the schematic picture of  $4 \times 4$  period double- $\mathbf{q}$  BO with  $\mathbf{Q}_1 = (\pi/2, 0)$  and  $\mathbf{Q}_2 = (0, \pi/2)$ . Hereafter, we set  $\delta t_0 = 0.075$  and  $T_{\text{BO}} = 0.02$  to follow the BCS universal ratio between the gap size and the transition temperature as we will explain later. From  $|t_1| \simeq 0.5\text{eV}$  given by the first principle calculation [67],  $T_{\text{BO}} = 0.02 \simeq 120\text{K}$  is estimated.

We introduce the cluster-Hubbard models to consider the electronic states under the antiferro BO. The hopping Hamiltonian  $H_0$  can be rewritten by

$$H_0 = \sum_{\sigma} \sum_{lm\alpha\beta} t_{lm,\alpha\beta} a_{l\alpha\sigma}^{\dagger} a_{m\beta\sigma}, \quad (2)$$

where  $\alpha(\beta)$  is the site index in a unit cell  $l(m)$ . As shown in Fig. 1(e), a set of  $l$  and  $\alpha$  ( $m$  and  $\beta$ ) corresponds to a site  $i(j)$ .

We use the site-dependent FLEX approximation to calculate the spin susceptibility  $\hat{\chi}^s(q) = \hat{\chi}^0(q) [1 - U \hat{\chi}^0(q)]^{-1}$  in the cluster models, where  $\hat{\chi}^0(q)$  is the irreducible susceptibility.  $\hat{\chi}^s(q)$  and  $\hat{\chi}^0(q)$  are  $4 \times 4$  matrices for the single- $\mathbf{q}$  ( $16 \times 16$  matrices for the double- $\mathbf{q}$ ) case. We use the short notations  $k = (\mathbf{k}, i\varepsilon_n)$  and  $q = (\mathbf{q}, i\omega_l)$ , where  $\varepsilon_n$  and  $\omega_l$  are fermion and boson Matsubara frequencies, respectively. We ignore the modulation in the FS shape by the FLEX self-energy, approximately, as we explain in SM. A.

Here, we explain the “unfolding” procedure [68]. A physical quantity under the antiferro order in Fig. 1 (e) is expressed as  $A(\mathbf{r}_i - \mathbf{r}_j) = A_{\alpha\beta}(\mathbf{R}_l - \mathbf{R}_m)$ , and its Fourier transformation is  $A_{\alpha\beta}(\mathbf{k}) = \sum_l A_{\alpha\beta}(\mathbf{R}_l) \exp\{-i(\mathbf{k} \cdot \mathbf{R}_l)\}$ . Here,  $\mathbf{R}_l$  is the position of the unit cell  $l$ , and we put  $-\pi < k_x, y \leq \pi$ . Then, its average is given as

$$A(\mathbf{k}) = \frac{1}{N_c} \sum_{\alpha\beta} A_{\alpha\beta}(\mathbf{k}) e^{-i\mathbf{k} \cdot (\boldsymbol{\tau}_{\alpha} - \boldsymbol{\tau}_{\beta})}, \quad (3)$$

where  $N_c$  is the number of the sites in a unit cell, and  $\boldsymbol{\tau}_{\alpha}$  is the position of the site  $\alpha$ . The obtained  $A(\mathbf{k})$  is unfolded to the single-site Brillouin zone because the translational symmetry is recovered approximately.

Figure 1(f) shows the real part of the spin susceptibility  $\text{Re}\chi^s(\mathbf{q}, 0)$  without the BO at  $T = 0.01$  for  $U = 4.75$ .  $\text{Re}\chi^s(\mathbf{q}, 0)$  has the peak at  $\mathbf{Q}_s = (\pi, \pi)$  due to the nesting shown in Fig. 1(b).

Figure 2(a) shows the  $T$  dependence of the DOS under the single- $\mathbf{q}$  BO without the FLEX self-energy. We estimate the bare (: without the FLEX self-energy) gap size

$2\Delta_{\text{BO}}$  from the width between the peaks of the DOS. Note that the relation between  $\Delta_{\text{BO}}(T)$  and  $\delta t(T)$  is  $2\Delta_{\text{BO}}(T) \simeq 4\delta t(T)$  under the single- $\mathbf{q}$  BO. (The DOS under  $s$ -wave and  $s'$ -wave orders is discussed in SM. D.) This relation can be understood from the inter-band hybridization due to the band holding [49, 69] (see SM. B.). In Fig. 2(b), we compare the DOS under the single- $\mathbf{q}$  BO with the DOS under the double- $\mathbf{q}$  one. The decrease in the DOS is larger in the double- $\mathbf{q}$  case. To compare with experiments, we calculate the renormalized gap as  $2\Delta_{\text{BO}}^*(\mathbf{k}, T) = 2\Delta_{\text{BO}}(T)/Z(\mathbf{k}, T)$ , where  $Z(\mathbf{k}, T) = \left[1 - \frac{\Sigma(\mathbf{k}, i\pi T) - \Sigma(\mathbf{k}, -i\pi T)}{2i\pi T}\right]$  is the mass enhancement factor due to the FLEX self-energy  $\Sigma(k)$ . We obtain  $Z(\mathbf{k}, T) \simeq 4.5$  for  $\mathbf{k} = (\pi, 0)$  at  $T = 0.01$ . Therefore, we obtain the relation  $\Delta_{\text{BO}}^*(T = 0)/T_{\text{BO}} \simeq 1.7$  for  $\delta t_0 = 0.075$  and  $T_{\text{BO}} = 0.02$  under the single- $\mathbf{q}$  BO. It is almost the same as the BCS universal ratio. Note that  $\Delta_{\text{BO}}^*(T = 0)/T_{\text{BO}} \simeq 3$  is observed in Hg-based and Y-based cuprates by the Raman spectroscopy [70].

Figures 2(c) and (d) show the FS with the unfolded spectral function under the single- $\mathbf{q}$  and the double- $\mathbf{q}$  BOs, respectively. The unfolded spectral function is obtained by  $\rho(\mathbf{k}, \omega) = -\frac{1}{\pi} \frac{1}{N_c} \sum_{\alpha\beta} \text{Im}G_{\alpha\beta}^0(\mathbf{k}, \omega) e^{-i\mathbf{k}\cdot(\mathbf{r}_\alpha - \mathbf{r}_\beta)}$  according to Eq. (3), where  $G_{\alpha\beta}^0(\mathbf{k}, \omega)$  is the retarded bare Green function.

The band-hybridization gap induces the Fermi arc structure. The FS near  $\mathbf{k} = (0, \pm\pi)$  vanishes and has  $C_2$  symmetry under the single- $\mathbf{q}$  BO as shown in Fig. 2 (d), so the electronic nematic response should appear. On the other hand, the FS near  $\mathbf{k} = (0, \pm\pi), (\pm\pi, 0)$  vanishes and has the  $C_4$  symmetry under the double- $\mathbf{q}$  BO shown in Fig. 1 (d) as shown in Fig. 2 (d). Interestingly, the FS under the double- $\mathbf{q}$  BO possesses the  $C_4$  symmetry for any phase parameters  $\gamma$  of two BOs, and therefore electronic nematic response is unexpected. The Fermi arc structure in Fig. 2(d) was actually observed by ARPES measurements [71–74]. Even in the single- $\mathbf{q}$  case, if the BO has small domain structures, the Fermi arc structure similar to Fig. 2(d) would be also observed since the FS shown in Fig. 2(c) and its 90 degree rotation are averaged. Observed domain size is typically a few nm [25, 31–34]. Therefore, the experimental Fermi arc can be explained by both single- $\mathbf{q}$  and double- $\mathbf{q}$  BOs.

Next, we study  $\hat{\chi}^s(\mathbf{q})$  with the four-period  $d$ -wave BO. Figures 3(a) and (b) show the local DOS  $\rho_\alpha(\omega) = -\frac{1}{\pi} \sum_{\mathbf{k}} \text{Im}G_{\alpha\alpha}^0(\mathbf{k}, \omega)$  and  $\text{Re}\chi_{\alpha\alpha}^s(\mathbf{q}, 0)$  for  $\mathbf{q} = (\pi, q_y)$ , respectively.  $\alpha$  represents the site-numbers in Fig. 1(c). For  $\gamma = 0$  in Eq. (1), the components of the  $\alpha = 2$  and  $\alpha = 4$  are equivalent, and there are three inequivalent components. We also show that there are two inequivalent components for  $\gamma = \pi/4$  in Fig. S1(b) and (c) in SM. Such local site-dependence has been observed as the broadening of the NMR signal [75].

Figure 3(c) shows the  $T$  dependence of  $1/(1 - \alpha_s)$ , where  $\alpha_s$  is the maximum eigenvalue of  $U\hat{\chi}^0(\mathbf{q}, 0)$ , and a

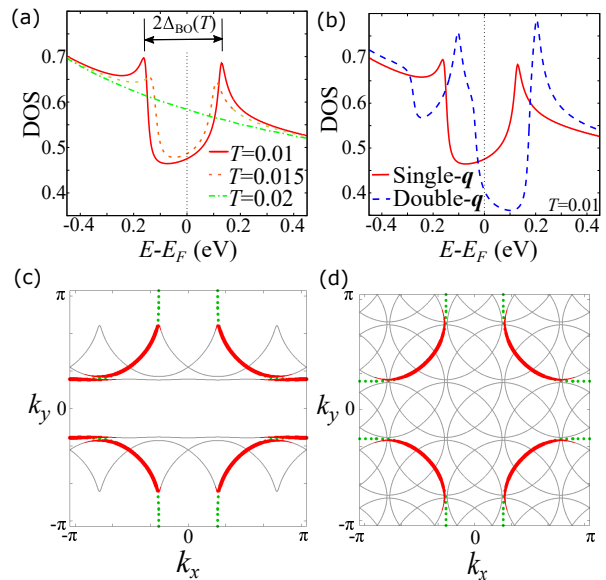


FIG. 2. (a)  $T$  dependence of the DOS under the single- $\mathbf{q}$  BO. (b) DOS under the single- $\mathbf{q}$  and the double- $\mathbf{q}$  BOs at  $T = 0.01$ . (c) Unfolded FS under the single- $\mathbf{q}$  BO (thick red lines) and the folded FS (thin gray lines) under the bond order. The green dotted lines represent the vanished FS due to the BO. (d) Folded and unfolded FSs under the double- $\mathbf{q}$  BO.

magnetic transition emerges when  $\alpha_s$  reaches unity because  $\hat{\chi}^s(\mathbf{Q}_s, 0)$  diverges. Figure 3(d) shows the  $T$  dependence of  $1/T_1T$  given by

$$1/T_1T \propto \frac{1}{N_c} \sum_{\alpha\beta} \sum_{\mathbf{q}} \lim_{\omega \rightarrow 0} \frac{\text{Im}\chi_{\alpha\beta}^s(\mathbf{q}, \omega)}{\omega} e^{-i\mathbf{q}\cdot(\mathbf{r}_\alpha - \mathbf{r}_\beta)}. \quad (4)$$

Both  $1/T_1T$  and  $\alpha_s$  decrease with decreasing  $T$  below  $T_{\text{BO}}$  due to the Fermi arc structure. The decrease in  $\alpha_s$  due to the single- $\mathbf{q}$  BO is tiny maybe because the FS connected by the nesting vector  $\mathbf{Q}_s$  in Fig. 1(b) remains below  $T_{\text{BO}}$ . In a two-dimensional Fermi liquid, the relation between  $1/T_1T$  and  $\alpha_s$  is given by  $1/T_1T \propto N^2(0) \frac{1}{1 - \alpha_s}$  for  $T \simeq 0$  [76–78], where  $N(0)$  is the DOS at the Fermi energy  $E_F$ . This equation indicates that  $1/T_1T$  decreases in proportion to  $N(0)^2$  even if the change of  $\alpha_s$  is small.

In Fig. 3(d), theoretical  $1/T_1T$  shows a kink-type pseudogap, whereas experimental  $1/T_1T$  exhibits a broad peak [64]. This fact may indicate the existence of inhomogeneity in the BO state due to its short correlation length [20, 25, 29]. Note that the kink-behavior in Fig. 3(d) becomes moderate when  $\Delta_{\text{BO}}^*(T = 0)/T_{\text{BO}}$  is smaller or when  $\alpha_s$  is larger at  $T = T_{\text{BO}}$ . We have also verified that the present numerical results for the four-period BO are essentially similar to the results in the five-period BO case.

We discuss the relation between  $1/T_1T$  and  $\alpha_s$  in more detail. Figures 3(e) and (f) show the real and imaginary parts of unfolded  $\chi^s(\mathbf{Q}_s, \omega)$  for at  $T = 0.01$ ,

respectively.  $1/(1 - \alpha_s)$  is proportional to  $\chi^s(\mathbf{Q}_s, 0)$ , while  $1/T_1T$  reflects the slope of  $\text{Im}\chi^s(\mathbf{Q}_s, \omega)$  for  $\omega \simeq 0$ . As shown in Fig. 3(f),  $\text{Im}\chi^s(\mathbf{Q}_s, \omega)$  is suppressed for  $\omega \lesssim 2\Delta_{\text{BO}}^*$ , and its slope for small  $\omega$  decreases.  $\text{Im}\chi^s(\mathbf{q}, \omega) \simeq \frac{\text{Im}\chi^0(\mathbf{q}, \omega)}{(1 - U\chi^0(\mathbf{q}, 0))^2}$  is satisfied for small  $\omega$ , where  $\chi^0(\mathbf{q}, \omega)$  is the unfolded irreducible susceptibility. It is known that  $\text{Im}\chi^0(\mathbf{q}, \omega)$  is suppressed by a gap  $\Delta_{\text{BO}}^*$  for  $\omega \lesssim 2\Delta_{\text{BO}}^*$ .  $\text{Re}\chi^s(\mathbf{q}, \omega)$  and  $\text{Im}\chi^s(\mathbf{q}, \omega)$  are combined through the Kramers-Kronig relation  $\text{Re}\chi^s(\mathbf{q}, \omega) = \frac{1}{\pi} \text{P} \int_{-\infty}^{\infty} \frac{\text{Im}\chi^s(\mathbf{q}, \omega')}{\omega' - \omega} d\omega'$ . Since  $\text{Re}\chi^s(\mathbf{q}, \omega)$  is obtained by  $\omega$  integral of  $\text{Im}\chi^s(\mathbf{q}, \omega)$ , the low-energy suppression of  $\text{Im}\chi^s(\mathbf{Q}_s, \omega)$  by the BO does not reduce  $\text{Re}\chi^s(\mathbf{q}, \omega)$  largely, except for the close vicinity of the magnetic quantum critical point. Therefore, the change of  $\alpha_s$  is small irrespectively of the large decrease in  $1/T_1T$ .

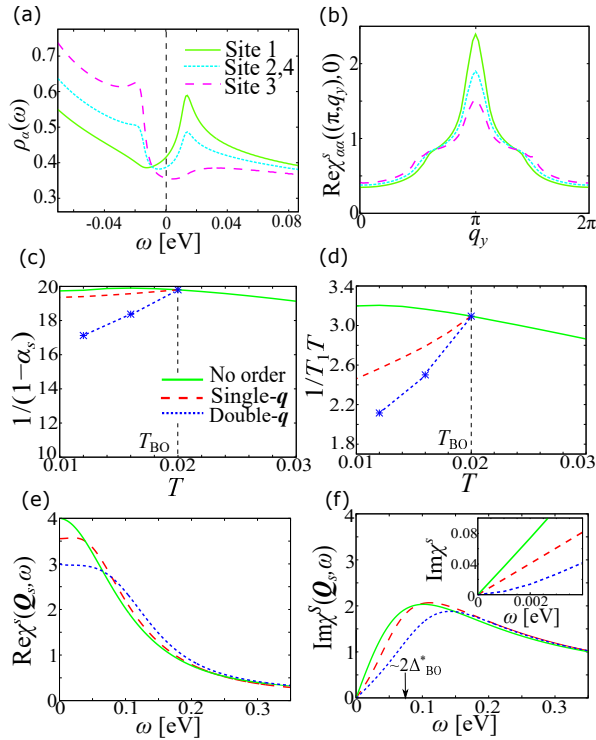


FIG. 3. (a)  $\rho_\alpha(\omega)$  and (b)  $\chi_{\alpha\alpha}^s((\pi, q_y), 0)$ . The site numbers are defined in Fig. 1(c). (c)  $T$  dependences of  $1/(1 - \alpha_s)$  and (d) that of  $1/T_1T$ . The solid, dashed, and dotted lines are no-order, single- $\mathbf{q}$ , and double- $\mathbf{q}$  BOs, respectively. (e)  $\text{Re}\chi^s(\mathbf{Q}_s, \omega)$  and (f)  $\text{Im}\chi^s(\mathbf{Q}_s, \omega)$  as a function of  $\omega$  at  $T = 0.01$ . The inset shows  $\text{Im}\chi^s(\mathbf{Q}_s, \omega)$  for the small  $\omega$  region.

Finally, we study the superconducting state by solving the linearized Eliashberg equation defined by

$$\lambda \Delta_{\alpha\beta}(k) = - \frac{T}{N} \sum_{k'\alpha'\beta'} G_{\alpha\alpha'}(k') \Delta_{\alpha'\beta'}(k') G_{\beta\beta'}(-k') \times V_{\alpha\beta}^{\text{sc}}(k - k'), \quad (5)$$

where  $V_{\alpha\beta}^{\text{sc}}(q) = \frac{3}{2}U^2\chi_{\alpha\beta}^s(q) - \frac{1}{2}U^2\chi_{\alpha\beta}^c(q) + U\delta_{\alpha\beta}$  is the singlet pairing interaction [79, 80]. Here,  $\lambda$  is the eigen-

value, and  $\Delta_{\alpha\beta}(k)$  is the superconducting gap function.  $N$  is the total number of the unit cells. At  $T = T_c$ ,  $\lambda = 1$  is satisfied. Figure 4 shows the  $T$  dependence of  $\lambda$ . We obtain  $T_c = 0.0134 \simeq 80$  K without the BO and  $T_c = 0.0116$  in the single- $\mathbf{q}$  BO. It means that  $T_c$  is suppressed only slightly (of order 10 K) due to the Fermi arc structure caused by the antiferro  $d$ -wave BO. The suppression of  $T_c$  by double- $\mathbf{q}$  BO is about twice of that by the single- $\mathbf{q}$  BO. These suppressions of  $T_c$  are consistent with the experimental phase diagrams. [27–30, 35].

In the present study, the site dependent electronic states under the BO are seriously analyzed. To verify that the site dependent analyses are important, we perform another calculation method, the SAA, in which calculations are performed based on the single-site model by using the unfolded bare Green function  $G^0(k)$ . The eigenvalue  $\lambda$  obtained by the SAA under the single- $\mathbf{q}$  BO is significantly underestimated as explained in Fig. 4. Also, both  $1/T_1T$  and  $1/(1 - \alpha_s)$  are underestimated in the SAA as shown in Fig. S2(a) and (b). It is because the site dependence of spin susceptibility shown in Fig. 3(b) is averaged in the SAA. Therefore, it is important to calculate the cluster-Hubbard model as performed in the present study.

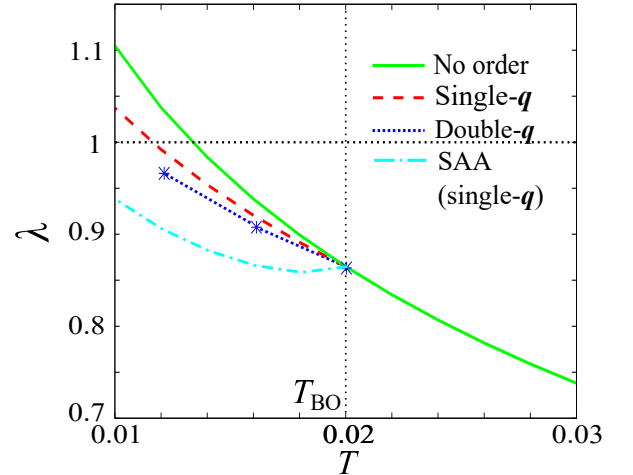


FIG. 4.  $T$  dependence of the eigenvalue  $\lambda$  of the linearized Eliashberg equation. The solid, dashed, and dotted lines correspond to no-order, single- $\mathbf{q}$  BO, and double- $\mathbf{q}$  BO, respectively. The dashed-dotted line represents  $\lambda$  given by the SAA for the single- $\mathbf{q}$  BO.

In summary, we studied the many-body electronic states to understand the CDW phase in Fig. 1(a). Based on the cluster Hubbard model with the finite  $d$ -wave BO, we analyzed  $\hat{\chi}^s(\mathbf{q}, \omega)$ ,  $1/T_1T$ , and  $T_c$  by using the site-dependent FLEX approximation. We found that the strong suppression of  $1/T_1T$  is induced by the BO while the decrease of  $\alpha_s$  is tiny, consistently with experiments [64, 65]. We also found a slight decrease of  $d$ -wave  $T_c$  about 10K under the BO, which is also consistent with the experiments [21, 27–30]. Since  $T_c$  and spin fluctua-

tions in the antiferro BO are significantly underestimated by using the SAA, site dependence must be taken into account seriously. This study supports the axial  $d$ -wave bond BO scenario in cuprates, where  $T_{BO}$  corresponds to  $T_{CDW}$  in Fig. 1(a).

This work was supported by the “Quantum Liquid Crystals” No. JP19H05825 KAKENHI on Innovative Areas from JPSJ of Japan, and JSPS KAKENHI (JP18H01175, JP20K03858, JP17K05543).

- 
- [1] D. Senechal and A.-M.S. Tremblay, Phys. Rev. Lett. **92**, 126401 (2004).
- [2] B. Kyung, S. S. Kancharla, D. Senechal, A. -M. S. Tremblay, M. Civelli, and G. Kotliar, Phys. Rev. B **73**, 165114 (2006).
- [3] T.A. Maier, M.S. Jarrell, and D.J. Scalapino, Physica C, **460-462**, 13 (2007).
- [4] A. Shekhter, B. J. Ramshaw, R. Liang, W. N. Hardy, D. A. Bonn, F. F. Balakirev, R. D. McDonald, J. B. Betts, S. C. Riggs, and A. Migliori, Nature 498, **75** (2013).
- [5] R.-H. He, M. Hashimoto, H. Karapetyan, J. D. Koralek, J. P. Hinton, J. P. Testaud, V. Nathan, Y. Yoshida, H. Yao, K. Tanaka, W. Meevasana, R. G. Moore, D. H. Lu, S.-K. Mo, M. Ishikado, H. Eisaki, Z. Hussain, T. P. Devereaux, S. A. Kivelson, J. Orenstein, A. Kapitulnik, and Z.-X. Shen, Science **331**, 1579 (2011).
- [6] Y. Sato S. Kasahara, H. Murayama, Y. Kasahara, E.- G. Moon, T. Nishizaki, T. Loew, J. Porras, B. Keimer, T. Shibauchi, and Y. Matsuda, Nat. Phys. **13**, 1074 (2017).
- [7] B. Fauqué, Y. Sidis, V. Hinkov, S. Pailhès, C. T. Lin, X. Chaud, and P. Bourges, Phys. Rev. Lett. **96**, 197001 (2006).
- [8] M. Tsuchiizu, K. Kawaguchi, Y. Yamakawa, and H. Kontani, Phys. Rev. B **97**, 165131 (2018).
- [9] K. Kawaguchi, M. Tsuchiizu, Y. Yamakawa, and H. Kontani, J. Phys. Soc. Jpn. **86**, 063707 (2017).
- [10] Y. Yamakawa and H. Kontani, Phys. Rev. Lett. **114**, 257001 (2015).
- [11] H. Kontani, Y. Yamakawa, R. Tazai, and S. Onari, Phys. Rev. Research **3**, 013127 (2021).
- [12] C. M. Varma, Phys. Rev. B **55**, 14554 (1997).
- [13] I. Affleck and J. B. Marston, Phys. Rev. B **37**, 3774(R) (1988).
- [14] F. C. Zhang, Phys. Rev. Lett. **64**, 974 (1990).
- [15] R. Tazai, Y. Yamakawa, and H. Kontani, arXiv:2010.16109.
- [16] G. Ghiringhelli, M. L. Tacon, M. Minola, S. Blanco-Canosa, C. Mazzoli, N. B. Brookes, G. M. D. Luca, A. Frano, D. G. Hawthorn, F. He, T. Loew, M. M. Sala, D. C. Peets, M. Salluzzo, E. Schierle, R. Sutarto, G. A. Sawatzky, E. Weschke, B. Keimer, and L. Braicovich, Science **337**, 821 (2012).
- [17] J. Chang, E. Blackburn, A. T. Holmes, N. B. Christensen, J. Larsen, J. Mesot, R. Liang, D. A. Bonn, W. N. Hardy, A. Watenphul, M. v. Zimmermann, E. M. Forgan, and S. M. Hayden, Nat. Phys. **8**, 871 (2012).
- [18] E. Blackburn, J. Chang, M. Hücker, A. T. Holmes, N. B. Christensen, R. Liang, D. A. Bonn, W. N. Hardy, U. Rütt, O. Gutowski, M. v. Zimmermann, E. M. Forgan, and S. M. Hayden, Phys. Rev. Lett. **110**, 137004 (2013).
- [19] M. Hücker, M. v. Zimmermann, G. D. Gu, Z. J. Xu, J. S. Wen, G. Xu, H. J. Kang, A. Zheludev, and J. M. Tranquada, Phys. Rev. B **83**, 104506 (2011).
- [20] F. Boschini, M. Minola, R. Sutarto, E. Schierle, M. Bluschke, S. Das, Y. Yang, M. Michiardi, Y. C. Shao, X. Feng, S. Ono, R. D. Zhong, J. A. Schneeloch, G. D. Gu, E. Weschke, F. He, Y. D. Chuang, B. Keimer, A. Damascelli, A. Frano, and E. H. da Silva Neto, Nat. Commun. **12**, 597 (2021).
- [21] E. H. da Silva Neto, P. Aynajian, A. Frano, R. Comin, E. Schierle, E. Weschke, A. Gyenis, J. Wen, J. Schneeloch, Z. Xu, S. Ono, G. Gu, M. L. Tacon, and A. Yazdani, Science **343**, 393 (2014).
- [22] R. Comin and A. Damascelli, Annu. Rev. Condens. Matter Phys. **7**, 369 (2016).
- [23] R. Comin, R. Sutarto, F. He, E. da Silva Neto, L. Chauviere, A. Frano, R. Liang, W. N. Hardy, D. Bonn, Y. Yoshida, H. Eisaki, J. E. Hoffman, B. Keimer, G. A. Sawatzky, and A. Damascelli, Nat. Mater. **14**, 796 (2015).
- [24] R. Comin, A. Frano, M. M. Yee, Y. Yoshida, H. Eisaki, E. Schierle, E. Weschke, R. Sutarto, F. He, A. Soumyanarayanan, Y. He, M. L. Tacon, I. S. Elfimov, J. E. Hoffman, G. A. Sawatzky, B. Keimer, and A. Damascelli, Science **343**, 390 (2014).
- [25] W. Tabis, B. Yu, I. Bialo, M. Bluschke, T. Kolodziej, A. Kozłowski, E. Blackburn, K. Sen, E. M. Forgan, M. v. Zimmermann, Y. Tang, E. Weschke, B. Vignolle, M. Heping, H. Gretarsson, R. Sutarto, F. He, M. Le Tacon, N. Barišić, G. Yu, and M. Greven, Phys. Rev. B **96**, 134510 (2017).
- [26] R. Arpaia, S. Caprara, R. Fumagalli, G. De Vecchi, Y. B. Peng, E. Andersson, D. Betto, G. M. De Luca, N. B. Brookes, F. Lombardi, M. Salluzzo, L. Braicovich, C. Di Castro, M. Grilli, G. Ghiringhelli, Science **365**, 6456 (2019).
- [27] W. Tabis, Y. Li, M. L. Tacon, L. Braicovich, A. Kreyssig, M. Minola, G. Dellea, E. Weschke, M. J. Veit, M. Ramazanoglu, A. I. Goldman, T. Schmitt, G. Ghiringhelli, N. Barišić, M. K. Chan, C. J. Dorow, G. Yu, X. Zhao, B. Keimer, and M. Greven, Nat. Commun. **5**, 5875 (2014).
- [28] M. Hücker, N. B. Christensen, A. T. Holmes, E. Blackburn, E. M. Forgan, Ruixing Liang, D. A. Bonn, W. N. Hardy, O. Gutowski, M. v. Zimmermann, S. M. Hayden, and J. Chang, Phys. Rev. B **90**, 054514 (2014).
- [29] S. Blanco-Canosa, A. Frano, E. Schierle, J. Porras, T. Loew, M. Minola, M. Bluschke, E. Weschke, B. Keimer, and M. Le Tacon, Phys. Rev. B **90**, 054513 (2014).
- [30] Naman K. Gupta, C. McMahan, R. Sutarto, T. Shi, R. Gong, Haofei I. Wei, K. M. Shen, F. He, Q. Ma, M. Dragomir, B. D. Gaulin, D. G. Hawthorn, arXiv:2012.08450.
- [31] K. Fujita, M. Hamidian, S. Edkins, C. Kim, Y. Kohsaka, M. Azuma, M. Takano, H. Takagi, H. Eisaki, S. Uchida, A. Allais, M. J. Lawler, E. -A. Kim, S. Sachdev, and J. C. S. Davis, Proc. Natl. Acad. Sci. U.S.A. **111**, E3026 (2014).
- [32] T. Hanaguri, C. Lupien, Y. Kohsaka, D.-H. Lee, M. Azuma, M. Takano, H. Takagi, and J. C. Davis, Nature **430**, 1001 (2004).
- [33] Y. Kohsaka, T. Hanaguri, M. Azuma, M. Takano, J. C. Davis, and H. Takagi, Nat. Phys. **8**, 534 (2012).
- [34] M. J. Lawler, K. Fujita, J. Lee, A. R. Schmidt, Y. Kohsaka, C. K. Kim, H. Eisaki, S. Uchida, J. C. Davis, J. P. Sethna, and E.-A. Kim, Nature **466**, 347 (2010).
- [35] M. E. Barber, H. Kim, T. Loew, M. L. Tacon, M. Minola,

- M. Konczykowski, B. Keimer, A. P. Mackenzie, and C. W. Hicks, arXiv:2101.02923.
- [36] J. C. Davis and D.-H. Lee, Proc. Natl. Acad. Sci. USA **110**, 17623 (2013).
- [37] M. A. Metlitski and S. Sachdev, Phys. Rev. B **82**, 075128 (2010).
- [38] C. Husemann and W. Metzner, Phys. Rev. B **86**, 085113 (2012).
- [39] K. B. Efetov, H. Meier, and C. P´epin, Nat. Phys. **9**, 442 (2013).
- [40] S. Sachdev and R. La Placa, Phys. Rev. Lett. **111**, 027202 (2013).
- [41] V. Mishra and M. R. Norman, Phys. Rev. B **92**, 060507 (2015).
- [42] E. Berg, E. Fradkin, S. A. Kivelson, and J. M. Tranquada, New J. Phys. **11**, 115004 (2009).
- [43] P. A. Lee, Phys. Rev. X **4**, 031017 (2014).
- [44] E. Fradkin, S. A. Kivelson, and J. M. Tranquada, Rev. Mod. Phys. **87**, 457 (2015).
- [45] Y. Wang, D. F. Agterberg, and A. V. Chubukov, Phys. Rev. Lett. **114**, 197001 (2015).
- [46] S. Onari, Y. Yamakawa, and H. Kontani, Phys. Rev. Lett. **116**, 227001 (2016).
- [47] S. onari and H. Kontani, Phys. Rev. Lett. **109**, 137001 (2012).
- [48] Y. Yamakawa, S. Onari, and H. Kontani, Phys. Rev. X **6**, 021032 (2016).
- [49] R. Tazai, Y. Yamakawa, M. Tsuchiizu, and H. Kontani, arXiv:2010.15516.
- [50] S. Onari and H. Kontani, Phys. Rev. B **100**, 020507(R) (2019).
- [51] S. Onari and H. Kontani, Phys. Rev. Res. **2**, 042005(R) (2020).
- [52] W. Metzner, M. Salmhofer, C. Honerkamp, V. Meden, and K. Sch¨onhammer, Rev. Mod. Phys. **84**, 299 (2012).
- [53] C. Bourbonnais, B. Guay, and R. Wortis, in Theoretical Methods for Strongly Correlated Electrons, edited by D. S´en´echal, A.-M. Tremblay, and C. Bourbonnais (Springer, New York, 2004) pp. 77-137.
- [54] M. Tsuchiizu, Y. Ohno, S. Onari, and H. Kontani, Phys. Rev. Lett. **111**, 057003 (2013).
- [55] R. Tazai, Y. Yamakawa, M. Tsuchiizu, and H. Kontani, Phys. Rev. B **94**, 115155 (2016).
- [56] C. Honerkamp, *ibid.* **72**, 115103 (2005).
- [57] Y. Wang and A. V. Chubukov, Phys. Rev. B **90**, 035149 (2014).
- [58] R. tazai and H. Kontani, Phys. Rev. B **100**, 241103(R) (2019).
- [59] H. Kontani, Rep. Prog. Phys. **71** 026501 (2008).
- [60] H. Kontani, Transport Phenomena in Strongly Correlated Fermi Liquids (Springer-Verlag, Berlin, 2013).
- [61] Nicolas Doiron-Leyraud, S. Lepault, O. Cyr-Choini`ere, B. Vignolle, G. Grissonnanche, F. Lalibert´e, J. Chang, N. Barišić, M. K. Chan, L. Ji, X. Zhao, Y. Li, M. Greven, C. Proust, and Louis Taillefer, Phys. Rev. X **3**, 021019 (2013).
- [62] David LeBoeuf, Nicolas Doiron-Leyraud, Julien Levallois, R. Daou, J.-B. Bonnemaision, N. E. Hussey, L. Balicas, B. J. Ramshaw, Ruixing Liang, D. A. Bonn, W. N. Hardy, S. Adachi, Cyril Proust, Louis Taillefer, Nature **450**, 533 (2007).
- [63] F. Lalibert´e, J. Chang, N. Doiron-Leyraud, E. Hassinger, R. Daou, M. Rondeau, B.J. Ramshaw, R. Liang, D.A. Bonn, W.N. Hardy, S. Pyon, T. Takayama, H. Takagi, I. Sheikin, L. Malone, C. Proust, K. Behnia and Louis Taillefer, Nat. Commun. **2**, 432 (2011).
- [64] M. Takigawa, A. P. Reyes, P. C. Hammel, J. D. Thompson, R. H. Heffner, Z. Fisk, and K. C. Ott, PRB. **43**, 247 (1991).
- [65] M. K. Chan, C. J. Dorow, L. Mangin-Thro, Y. Tang, Y. Ge, M. J. Veit, G. Yu, X. Zhao, A. D. Christianson, J. T. Park, Y. Sidis, P. Steffens, D. L. Abernathy, P. Bourges and M. Greven, Nat. Commun. **7**, 10819 (2016).
- [66] N. E. Bickers and S. R. White, Phys. Rev. B **43**, 8044 (1991).
- [67] P.Hansmann, N. Parragh, A. Toschi, G. Sangiovanni, and K. Held, New J. Phys. **16** 033009 (2014).
- [68] W. Ku, T. Berlijn, and C. -C, Lee, Phys. Rev. Lett. **104**, 216401 (2010).
- [69] K. Seo, and S. Tewari, Phys. Rev. B **90**, 174503 (2014).
- [70] B. Loret, N. Auvray, Y. Gallais, M. Cazayous, A. Forget, D. Colson, M.-H. Julien, I. Paul, M. Civelli and A. Sacuto, Nat. Phys. **15**, 771-775(2019)
- [71] T. Yoshida, M. Hashimoto, I. M. Vishik, Z. -X. Shen and A. Fujimori, JPSJ. **81**, 011006(2012).
- [72] H. M. Fretwell, A. Kaminski, J. Mesot, J. C. Campuzano, I. M. R. Norman, M. Randeria, T. Sato, R. Gatt, T. Takahashi, and K. Kadowaki, Phys. Rev. Lett. **84**, 4449 (2000).
- [73] M. Vishik, Rep. Prog. Phys. **81** 062501 (2018).
- [74] B. Keimer, S. A. Kivelson, M. R. Norman, S. Uchida, and J. Zaanen, Nature **518**, 179-186 (2015).
- [75] S. Kawasaki, Z. Li, M. Kitahashi, C.T. Lin, P.L. Kuhns, A.P. Reyes, and Guo-qing Zheng, Nature **8**, 1267 (2017).
- [76] T. Moriya and K. Ueda, Adv. Phys. **49**, 555 (2000).
- [77] H. Shiba, PTP. **54**, 967 (1975).
- [78] K. Yamada, Electron Correlation in Metals (Cambridge University Press, Cambridge, U.K., 2004).
- [79] D. J. Scalapino, Phys. Rep. **250**, 329 (1995).
- [80] D. J. Scalapino, E. Loh, and J. E. Hirsch, Phys. Rev. B **34**, 8190 (1986).

[Supplementary Material]  
Development of spin fluctuations under the presence of  $d$ -wave bond order in cuprate superconductors

Satoshi Ando, Youichi Yamakawa, Seiichiro Onari, and Hiroshi Kontani

*Department of Physics, Nagoya University, Nagoya 464-8602, Japan*

**A: The site-dependent FLEX approximation in cluster Hubbard models**

We use the site-dependent FLEX approximation [1] to analyze  $\hat{\chi}^s(q)$  and  $T_c$  with the cluster Hubbard model. The FLEX self-energy  $\Sigma_{\alpha\beta}(k)$  is given by

$$\Sigma_{\alpha\beta}(k) = \frac{T}{N} \sum_{k'} V_{\alpha\beta}(k-k') G_{\alpha\beta}(k') \quad (\text{S1})$$

$$V_{\alpha\beta}(q) = \frac{3}{2} U^2 \chi_{\alpha\beta}^s(q) + \frac{1}{2} U^2 \chi_{\alpha\beta}^c(q). \quad (\text{S2})$$

We use the short notations  $k = (\mathbf{k}, i\varepsilon_n)$  and  $q = (\mathbf{q}, i\omega_l)$ , where  $\varepsilon_n$  and  $\omega_l$  are fermion and boson Matsubara frequencies, respectively.  $V_{\alpha\beta}(k)$  is the effective interaction in the FLEX approximation, and  $G_{\alpha\beta}(k)$  is the Green function defined by

$$G_{\alpha\beta}(\mathbf{k}, i\varepsilon_n) = \left[ i\varepsilon_n \hat{1} - \hat{H}(\mathbf{k}) - \hat{\Sigma}(\mathbf{k}, i\varepsilon_n) + \mu \hat{1} \right]_{\alpha\beta}^{-1}, \quad (\text{S3})$$

where the components of  $\hat{H}(\mathbf{k})$  is given by  $H_{\alpha\beta}(\mathbf{k}) = N^{-1} \sum_{lm} t_{lm,\alpha\beta} \exp(-i\mathbf{k} \cdot (\mathbf{R}_l - \mathbf{R}_m))$ . Here,  $\mathbf{R}_l(\mathbf{R}_m)$  is the position of the unit-cell  $l(m)$ .  $\chi_{\alpha\beta}^c(q)$  is the charge susceptibility defined by  $\chi_{\alpha\beta}^c(q) = [\hat{\chi}^0(q)(1 + U\hat{\chi}^0(q))^{-1}]_{\alpha\beta}$ , and  $\chi_{\alpha\beta}^s(q)$  is the spin susceptibility defined by  $\chi_{\alpha\beta}^s(q) = [\hat{\chi}^0(q)(1 - U\hat{\chi}^0(q))^{-1}]_{\alpha\beta}$ , where the irreducible susceptibility  $\chi_{\alpha\beta}^0(q)$  is defined by  $\chi_{\alpha\beta}^0(q) = -TN^{-1} \sum_{\mathbf{k}} G_{\alpha\beta}(\mathbf{k} + q) G_{\beta\alpha}(\mathbf{k})$ .  $N$  is the total number of the unit cells, and  $\mu$  is the chemical potential. We solve these Eqs. (S1)-(S3) self-consistently. In the present study, we subtract the static and Hermitian part of the self-energy “ $\Delta\Sigma_{\alpha\beta}(\mathbf{k})$ ” from  $\Sigma_{\alpha\beta}(k)$  to keep the shape of the Fermi surface.  $\Delta\Sigma_{\alpha\beta}(\mathbf{k})$  is given by  $\Delta\Sigma_{\alpha\beta}(\mathbf{k}) \equiv \frac{1}{2} [\Sigma_{\alpha\beta}(\mathbf{k}, 0_+) + \Sigma_{\alpha\beta}(\mathbf{k}, 0_-)]$ , where  $\Sigma_{\alpha\beta}(\mathbf{k}, 0_{\pm}) \sim \frac{3}{2} \Sigma_{\alpha\beta}(\mathbf{k}, \pm i\pi T) - \frac{1}{2} \Sigma_{\alpha\beta}(\mathbf{k}, \pm i3\pi T)$ .

**B: Independence of the phase of the anti ferro  $d$ -wave bond order**

In the main text, we set  $\gamma = 0$  as the phase of the bond order (BO) in Eq. (1). However, the effects of  $\gamma$  on the physical quantities are not trivial. Here, we also investigate the  $\gamma = \pi/4$  case. Figure S1(a) is the schematic picture of the four-period  $d$ -wave BO for  $\gamma =$

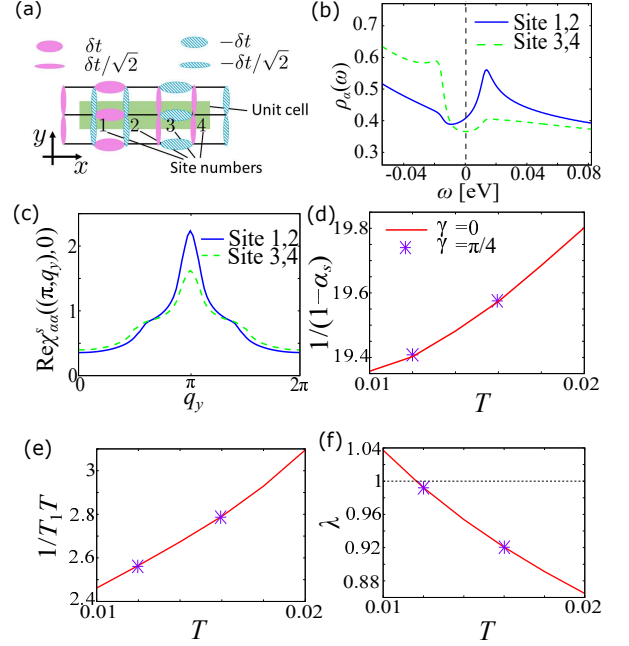


FIG. S1. (a) Schematic single- $\mathbf{q}$  four-period  $d$ -wave BO for  $\gamma = \pi/4$ .  $\delta t$  is the modulation of the hopping. (b)  $\rho_{\alpha}(\omega)$  and (c)  $\text{Re}\chi_{\alpha\alpha}^s((\pi, q_y), 0)$  for  $\gamma = \pi/4$  at  $T = 0.01$  (d)  $T$  dependence of  $1/(1 - \alpha_s)$ , (e) that of  $1/T_1 T$ , and (f) that of  $\lambda$  for  $\gamma = 0$  and  $\gamma = \pi/4$  under the single- $\mathbf{q}$  BO.

$\pi/4$ . Then, the local DOS  $\rho_{\alpha}(\omega)$  and  $\chi_{\alpha\alpha}^s((\pi, q_y), 0)$  have the site dependence and split into two lines as shown in Figs. S1(b) and (c), which are different from the results for  $\gamma = 0$  in the main text in Figs. 3(a) and (b). On the other hand, the total DOS in Fig. 2(a) for  $\gamma = 0$  is equivalent to that for  $\gamma = \pi/4$  completely. As shown in Fig. S1(d),  $\alpha_s$  also does not depend on  $\gamma$  in spite of the difference between  $\chi_{\alpha\alpha}^s$  for  $\gamma = 0$  in Fig. 3(c) and that for  $\gamma = \pi/4$ . Also,  $1/T_1 T$  and  $\lambda$  are independent on  $\gamma$  as shown in Figs. S1(e) and (f).

In the  $4 \times 1$  model, the dominant inter-band hybridization on the FS can be understood by a  $2 \times 2$  matrix. At  $\mathbf{k} = (0, \pm\pi)$ ,  $\mathbf{k} \pm \mathbf{Q}_1/2$  are on the FS as shown in Fig. 1 (b), and the band dispersions without order satisfy the relation  $\varepsilon_{\mathbf{k} \pm \mathbf{Q}_1/2} \approx \mu$ . The hybridization between  $\mathbf{k} - \mathbf{Q}_1/2$  and  $\mathbf{k} + \mathbf{Q}_1/2$  is represented by

$$\begin{pmatrix} \varepsilon_{\mathbf{k} - \mathbf{Q}_1/2} - \mu & \delta t_{\mathbf{k} - \mathbf{Q}_1/2, \mathbf{k} + \mathbf{Q}_1/2} \\ \delta t_{\mathbf{k} - \mathbf{Q}_1/2, \mathbf{k} + \mathbf{Q}_1/2}^* & \varepsilon_{\mathbf{k} + \mathbf{Q}_1/2} - \mu \end{pmatrix},$$

where  $\delta t_{\mathbf{k}-\mathbf{Q}_1/2, \mathbf{k}+\mathbf{Q}_1/2}$  is the band hybridization component due to the BO and is proportional to “ $d$ -wave form factor”, which is defined by

$$f_d(\mathbf{k}) \equiv \cos k_x - \cos k_y. \quad (\text{S4})$$

$\delta t_{\mathbf{k}-\mathbf{Q}_1/2, \mathbf{k}+\mathbf{Q}_1/2}$  is given by  $\delta t_{\mathbf{k}-\mathbf{Q}_1/2, \mathbf{k}+\mathbf{Q}_1/2} = N_c^{-1} \sum_{ij} \delta t_{ij}^{Q_1} \exp[i(\mathbf{k} - \mathbf{Q}_1/2) \cdot \mathbf{r}_i] \exp[-i(\mathbf{k} + \mathbf{Q}_1/2) \cdot \mathbf{r}_j] = \delta t f_d(\mathbf{k})$ . Then, the pseudogap opens due to  $|\delta t_{\mathbf{k}-\mathbf{Q}_1/2, \mathbf{k}+\mathbf{Q}_1/2}| = 2\delta t(T)$  at  $(0, \pm\pi)$ , and the gap size is  $2\Delta_{\text{BO}}(T) \simeq 4\delta t(T)$  as shown in Fig. 2 (a).  $|\delta t_{\mathbf{k}-\mathbf{Q}_1/2, \mathbf{k}+\mathbf{Q}_1/2}|$  does not depend on  $\gamma$ , therefore the total DOS is also independent on  $\gamma$ .

### C: Site-averaging approximation (SAA) results

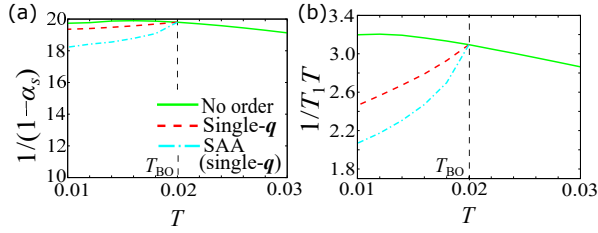


FIG. S2. (a)  $T$  dependence of  $1/(1 - \alpha_s)$  and (b) that of  $1/T_1 T$  obtained by the single- $\mathbf{q}$  BO and the SAA for the single- $\mathbf{q}$  BO.

In the site-averaging approximation (SAA) introduced in the main text, we use the unfolded bare Green function  $G^0(k)$ , which is the site-average of  $G_{\alpha\beta}^0(k) = \left[ (i\varepsilon_n \hat{1} - \hat{H}(\mathbf{k}) + \mu \hat{1})^{-1} \right]_{\alpha\beta}$  following Eq. (3).  $G^0(k)$  reproduces the total DOS shown in Fig. 2 (a) under the antiferro BOs, while the site-dependence is dropped. The SAA Green function is defined by

$$G_{\text{SAA}}(k) = G^0(k)/(1 - G^0(k)\Sigma_{\text{SAA}}(k)), \quad (\text{S5})$$

where  $\Sigma_{\text{SAA}}(k)$  is the single-site FLEX self-energy composed of  $G_{\text{SAA}}(k)$ . We solve  $G_{\text{SAA}}(k)$  in Eq. (S5) and  $\Sigma_{\text{SAA}}(k)$  self-consistently in the SAA-FLEX. In Fig. S2, we compare the results of the cluster model with those in the SAA for single- $\mathbf{q}$  BO. Figures S2(a) and (b) exhibit the obtained  $1/(1 - \alpha_s)$  and  $1/T_1 T$ , respectively. Both of them are underestimated in the SAA. In the same way,

$\lambda$  given by the SAA in Fig. 4 is prominently underestimated. Those underestimation come from the neglect of the site dependence in  $\chi_{\alpha\beta}^s$  in Fig. 3(b) or S1(c).

### D: DOS under the $s'$ -wave BO

We consider the two types  $s$ -wave form factors “ $f_{s'}(\mathbf{k}) \equiv \cos k_x + \cos k_y$ ” and “ $f_s(\mathbf{k}) \equiv 1$ ”. The

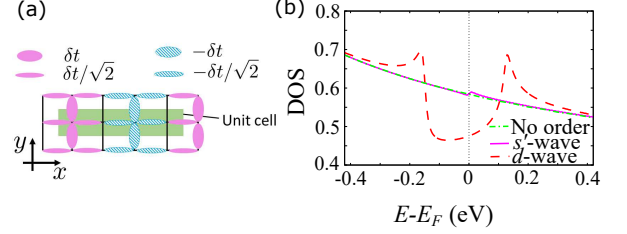


FIG. S3. (a) Schematic single- $\mathbf{q}$  four-period  $s'$ -wave BO.  $\delta t$  is the modulation of the hopping. (b) DOS under the single- $\mathbf{q}$   $s'$ -wave BO, the single- $\mathbf{q}$   $d$ -wave BO, and no-order at  $T = 0.01$ .

Fourier-transformation of them gives the  $s'$ -wave BO  $\delta t_{ij}^q \propto [\delta_{\mathbf{r}_i - \mathbf{r}_j, \hat{x}} + \delta_{\mathbf{r}_i - \mathbf{r}_j, \hat{y}} + (i \leftrightarrow j)] \text{Re}\{e^{-i(\mathbf{q} \cdot \frac{\mathbf{r}_i + \mathbf{r}_j}{2})}\}$  as shown in Fig. S3 (a) and the conventional CDW  $\delta t_{ij}^q \propto \delta_{\mathbf{r}_i, \mathbf{r}_j} \text{Re}\{e^{-i(\mathbf{q} \cdot \frac{\mathbf{r}_i + \mathbf{r}_j}{2})}\}$ , respectively. In the  $s'$ -wave BO case, the pseudogap is not induced as shown in Fig. S3 (b) because  $f_{s'}(\mathbf{k}) \propto \delta t_{\mathbf{k}-\mathbf{Q}_1/2, \mathbf{k}+\mathbf{Q}_1/2}$  is zero at  $(0, \pm\pi)$  and the relation  $\varepsilon_{\mathbf{k} \pm \mathbf{Q}_1/2} \approx \mu$  holds. The  $s'$ -wave BO is observed in La-based compound (LBCO) [2]. Our analysis for the  $s'$ -wave BO is consistent that apparent pseudogap have not been observed in LBCO. On the other hand, the conventional CDW with the local density modulation induces the pseudogap because  $f_s(\mathbf{k})$  has a finite value at  $(0, \pm\pi)$ . However, it is strongly suppressed by the on-site Coulomb interaction  $U$  and does not realize in cuprate superconductors.

- 
- [1] N. E. Bickers and S. R. White, Phys. Rev. B **43**, 8044 (1991).  
 [2] A. J. Achkar, F. He, R. Sutarto, Christopher McMahon, M. Zwiebler, M. Hücker, G. D. Gu, Ruixing Liang, D. A. Bonn, W. N. Hardy, J. Geck and D. G. Hawthorn, Nat. Mater. **15**, 616-620 (2016).